A R C H I V E S O F M E T A L L U R G Y A N D M A T E R I A L S
Volume 58 2013 Issue 4
DOI: 10.2478/amm-2013-0172

P. WAWRZAŁA*

# APPLICATION OF A PREISACH HYSTERESIS MODEL TO THE EVALUATION OF PMN-PT CERAMICS PROPERTIES

# ZASTOSOWANIE MODELU PREISACHA DO OPISU WŁAŚCIWOŚCI ELEKTROCERAMIKI PMN-PT

The work presents enhanced, relatively new iterative method for obtaining the classical Preisach distribution from a single, saturated hysteresis loop. As the material for research and analysis, the ceramic solid solution (1-$x$)Pb($Mg_{1/3}Nb_{2/3}$)$O_3$–$x$$PbTiO_3$ ($x$ = 0 to 0.40) was selected. Distributions were obtained for (1-$x$)PMN-$x$PT ceramics as a function of PT content, and function of temperature, for a selected composition from the morphotropic phase boundary region. The paper also proposes a mathematical model of the Preisach distribution and the parameters of the distribution were calculated. The typical factors achievable directly from the hysteresis loop with a coefficients determined from the analytical Preisach model were compared.

*Keywords*: ceramics, hysteresis, Preisach model, PMN-PT

Praca przedstawia rozszerzoną, relatywnie nową, iteracyjną metodę uzyskiwania klasycznego rozkładu Preisacha z pojedynczej, nasyconej pętli histerezy. Jako materiał do badań i analizy wybrano ceramiczny roztwór stały (1-$x$)Pb($Mg_{1/3}Nb_{2/3}$)$O_3$–$x$$PbTiO_3$ ($x$ = 0 do 0,40). Uzyskano matryce rozkładów Preisacha dla ceramik (1-$x$)PMN-$x$PT w funkcji zawartości PT oraz w funkcji temperatury dla wybranego składu z obszaru morfotropowego. Ponadto, zaproponowano matematyczny model dla dystrybucji Preisacha i wyznaczono parametry rozkładu. Porównano typowe współczynniki możliwe do uzyskania bezpośrednio z pętli histerezy z współczynnikami wynikającymi z analitycznego modelu Preisacha.

## 1. Introduction

The classical Preisach hysteresis model (CPM) [1], has been used widely to explain static hysteresis phenomenon in various ferroic materials. The CPM makes the following assumptions: the major hysteresis loop of a given ferromagnetic specimen consists of an infinite number of square hysteresis loops known as hysterons, and does not take into account stress, temperature dependence, frequency dependence, and so on. Each hysteron has associated threshold reversal fields up $E_\alpha$ and down $E_\beta$ as saturation magnetization switches from (+1) back to (-1) state as shown in Fig. 1. The mathematical form of the model can be written as:

$$x(t) = \iint\limits_{E\alpha \geqslant E\beta} \mu(E_\alpha, E_\beta)\gamma_{E\alpha E\beta}[u(t)]dE_\alpha dE_\beta \qquad (1)$$

where the weighing function $\mu(E_\alpha, E_\beta)$ is empirical and can be estimated by experiments and takes the form of a distribution matrix. It can be obtained by measuring the relaxation time or a set of reversal curves (FORC) [2]. But from the point of practical hysteresis numerical calculations, those two base methods are not efficient as the identification of distribution matrix are strongly dependent on the complicated and time-consuming experiments.

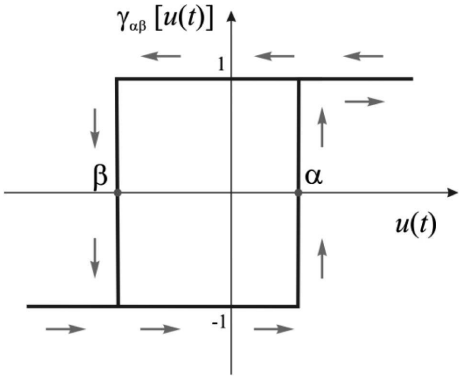


Fig. 1. Fundamental switching operator – hysteron

Obtained on the basis of experimental data (or assumed analytic functions) Preisach model allows the simulation of the material behavior in a variety of configurations of external electric fields. The most common use of CPM is linearization actuators answers containing materials exhibiting hysteresis as piezoelectrics, magnetics or shape memory alloys, for example [3], [4].

This paper presents method for obtaining Preisacha distribution based on the relatively new method of iteration [5]. It is also proposed the use of Preisach distributions analytical model to obtain additional information from the ferroelectric

* UNIVERSITY OF SILESIA, FACULTY OF COMPUTER SCIENCE AND MATERIALS SCIENCE MATERIALS SCIENCE DEPARTMENT, 2 ŚNIEŻNA STR., 41-200 SOSNOWIEC, POLAND

hysteresis loops, which are not easy to obtain from examining conventional parameters.

## 2. Experiment

Ceramic samples (1-x)PMN-xPT were obtained using sol-gel technology and densification was performed using uniaxial hot pressing method, as described in detail in previous paper [6]. X-ray diffraction patterns, fracture microphotographs, electromechanical parameters and hysteresis loops also to be found there, and the results of investigation of d.c. and a.c. conductivity were presented in [7]. For this study, using a Sawyer-Tower circuit, high voltage amplifier (HEOPS-5B6, Matsusada Precision Inc.) and computer with A/D, D/A transducers card (NI PCI-6014, National Instruments), hysteresis ($P(E)$) loops at triangular waveform a.c. electric field of $f = 1$ Hz were taken. Siemens D5000 X-ray diffractometer and Deby'e-Scherer method with filtrated $CuK_\alpha$ radiation have been used for structural investigations.

## 3. Iterative method of determining Preisach distribution

Developed procedure starts from ferroelectric hysteresis loops measured by mentioned above system. Then the hysteresis loop is split into two curves, the curve for increasing values of the electric field $P(E)_{inc}$ , and decreasing field curve for $P(E)_{dec}$ as illustrated in Fig. 2. In this work assumed a matrix $M$ consisting of $n = 100$ rows and columns (indices $r$ and $c$).

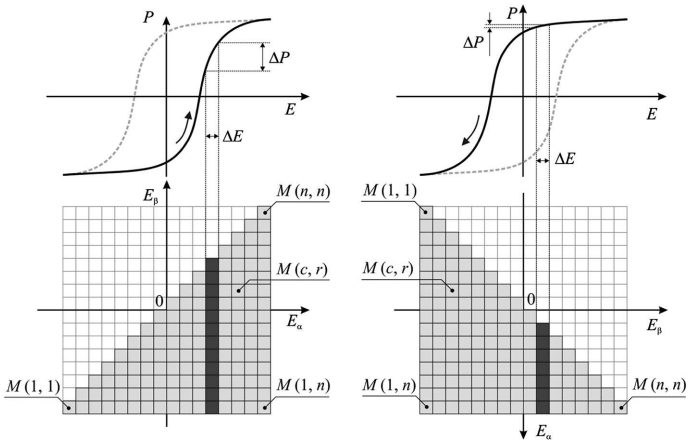


Fig. 2. Splitting the hysteresis loop into two curves, for increasing values of the electric field $P(E)_{inc}$ (left), and decreasing field curve for $P(E)_{dec}$ (right). Relation between $\Delta P_{inc}$ (left) and $\Delta P_{dec}$ (right) and Preisach distribution matrix element $M(c, r)$

The next step is optional, as it relates to filtering and smoothing of the experimental data $P(E)$. Actual waveforms by definition must contain some level of noise associated with concept of analog signal processing. Therefore, applying the derivative (first order) of the data, the associated noise is also amplified. In order to counteract this issue, in this work uses robust locally weighted regression of second degree (robust LOESS) [8]. The next phase of the procedure divides the curves $P(E)_{inc}$ and $P(E)_{dec}$ for $n$-sections. The purpose of this operation is to calculate for each range $1 \leqslant i \leqslant n$ values of $\Delta P_{inc}(i)$ and $\Delta P_{dec}(i)$ as the difference between two consecutive values of the polarization at the edges of the section. In the Preisach distribution matrix, the $\Delta P_{inc}(i)$ value corresponds with the sum of elements in a single column with index $c$, as shows the drawing of Fig. 2 left. Similarly, the polarization curve for decreasing field, the $\Delta P_{dec}(i)$ values refer to the sum of elements of $M(c, r)$ on a single line with index $r$ – Fig. 2 (right). These relationships can be written as:

$$\begin{aligned} \Delta P_{inc}(c) &= \sum_{r=1}^{c} M(c,r) \,, \\ \Delta P_{dec}(r) &= \sum_{c=k}^{n} M(c,r) \,. \end{aligned} \tag{2}$$

Moreover, it is easy to note that increasing and reducing the intensity of the electric field, the total polarization in both phases must be the same as the loop is closed (one of the objectives of CPM). Therefore, this relationship can provide:

$$\sum_{c} \Delta P_{inc}(c) = \sum_{r} \Delta P_{dec}(r) = P_{agg} \,. \tag{3}$$

The next step in the procedure is to initialize the Preisach array – the matrix corresponding to the weighting function. The matrix is filled according to the following formula:

$$M(c,r) = \begin{cases} P_{agg}/n(n+1) & (c \leqslant r), \\ 0 & (r < k). \end{cases} \tag{4}$$

An essential part of the achieving Preisach distribution procedure is the iteration process, which modifies the $M(c, r)$ matrix, in the range of $c, r \in \langle 1 \,, n \rangle$ variation, so that the following equations become true (with some, established accuracy):

$$\sum_{r=1}^{c} M(c,r) \cong \Delta P_{inc}(c) \,, \tag{5}$$

$$\sum_{c=r}^{n} M(c,r) \cong \Delta P_{dec}(r) \,. \tag{6}$$

Modified the $M$ array elements are stored in a $M_{adj}$ matrix. The first modification is the column of the matrix, so as to ensure the condition (4), according to the equation:

$$M_{adj}(c,r) = M(c,r) + \frac{\Delta P_{inc}(c) - \sum_{r=1}^{c} M(c,r)}{c} \,, \tag{7}$$

assuming that when the $M_{adj}(c, r) < 0$, it is stored as a zero value, due to the fact that the distribution function is always positive. Before attempting to modify the elements of the matrix in rows to fill the condition (5), the $M$ array is refreshed as:

$$M(c,r) = M_{adj}(c,r) \,. \tag{8}$$

Afterward, the matrix elements are changed for all $r$ according to the formula:

$$M_{adj}(c,r) = M(c,r) + \frac{\Delta P_{dec}(r) - \sum_{c=r}^{n} M(c,r)}{n - r + 1} \,. \tag{9}$$

Changed $M_{adj}$ matrix not fulfill the condition (3), so procedure is refreshing array according to equation (8) and repeat the process for the columns and rows. Repeating the last steps

(represented by 6-8 equations) can be seen that the difference between the matrices $M$ and $M_{adj}$ tends to zero. A convenient condition for the decision of when to stop the iteration process is the observation of the sum of squared residuals between the measured and calculated according to the model is widely used in the Levenberg-Marquardt method. In this procedure, for a double iterations (for columns and rows), the condition has been formulated by the equation:

$$\chi = \sum_{c=1}^{n}\left[\Delta P_{inc}(c) - \sum_{r=1}^{c} M(c,r)\right]^2 + \sum_{r=1}^{n}\left[\Delta P_{dec}(r) - \sum_{c=r}^{n} M(c,r)\right]^2. \tag{10}$$

If the value of $\chi$ remains is less than desired accuracy value or constant, this means that for a $M(n,n)$ the best fit was obtained. Therefore, the loops simulated with Preisach distribution show very good agreement with the experimental loops. Fig. 3 illustrates an exemplary the hysteresis loop and contour plot of the calculated distribution.

In summary developed procedure has several advantages over the commonly used methods for the identification of Preisach distribution: uses a single measurement of the saturated hysteresis loop – increased accuracy of data acquisition; simple measurement system; the ability to perform multiple measurements at short intervals; there is no need for a second order differentiation of data – increased accuracy of the calculation; simple computational procedure – increased speed of calculation.

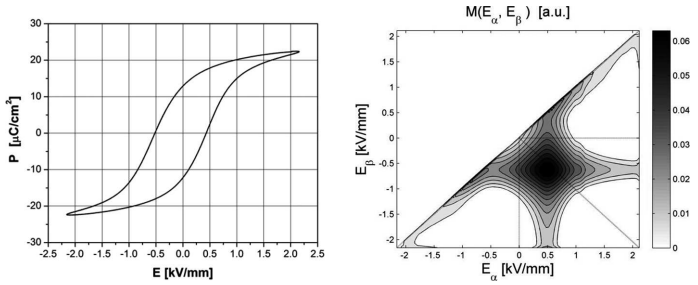


Fig. 3. Electric polarization ($P$) versus electric field ($E$) hysteresis loop for 0.775PMN-0.225PT sample at 70°C (left), and obtained Preisach matrix represented by density map (right)

## 4. Analytical model of a Preisach distribution

In many works can be found an analytical functions relating to modeling Preisach distributions resulting calculations and experimental measurements for ferroic materials. Most of them are modified three types of functions: Gaussian, Lorentz (Cauche) and log-normal distribution. While the for specific materials and conditions mentioned models functions describes loops with sufficient precision, unfortunately, with conditions changes, such as temperature, the accuracy of matching models is rapidly decreasing. This means that, for these models, it is not possible to find a set of parameters that will be in a wide range of changes in the sample properly describe material behaviour.

Sutor et al. [9] proposed distribution, which they called DAT (Derivate Arc Tangent):

$$\mu(E_\alpha, E_\beta) = \frac{A}{1 + \left\{ [(E_\alpha + E_\beta)\sigma_\alpha]^2 + \ [(E_\alpha - E_\beta - h)\sigma_\beta]^2 \right\}^n} \tag{11}$$

where: $A$ – parameter associated with the maximum value of the distribution, $\sigma_\alpha$, $\sigma_\beta$ – widths coefficients of the distribution, $h$ – shift of the distribution maximum, $n$ – coefficient characterizing the hardness of ferroelectric material. This function has been selected for further analysis because most precisely mapped distributions in a wide range of temperatures and compositions.

## 5. Results and discussion

Based on the above DAT distribution, numerically fits the model parameters to the Preisach matrix distributions determined from experimental data were made. DAT function has allowed to obtain high precision fit over the entire range of analyzes; coefficient of determination is not less than 0.83 for all fitted samples. As an example of the calculations, Fig. 4 shows temperature family of hysteresis loops of 0.690PMN-0.310PT ceramics, and corresponding, determined from loops remanent polarization, maximum polarization and coercive field. Fig. 5 shows corresponding Preisach distributions obtained using described earlier iterative method. The distribution of the parameters calculated with the DAT function for this sample as a function of temperature, and XRD line (200) decompositions at selected temperatures are presented in Fig. 6. The diffraction patterns decomposition has been performed using separating multipeak maxima standard method (built-in Lorentzian function in computer program Origin, OriginLab Corp.). Line (200) at some temperature ranges good results are obtained fitting with 4 maxima, at another ones with 2 maxima and at highest temperatures with 1 maximum, which indicates a change in the phase composition (sample belongs to compositions from morphotropic phase boundary region) [6], [10]. As may be seen power-law factor $n$ and width ratio $\sigma_\alpha$ of the distribution are fairly well reproduce temperature changes in the diffraction lines. The coefficients classically used to describe the hysteresis loops, like $E_C$, $P_R$, do not reproduce clearly the changes in the test samples (see Fig. 4). Since this phenomenon repeated for all tested compositions of PMN-PT, we can say that the particular factor $n$ in DAT distribution model is associated with structural changes in the material.

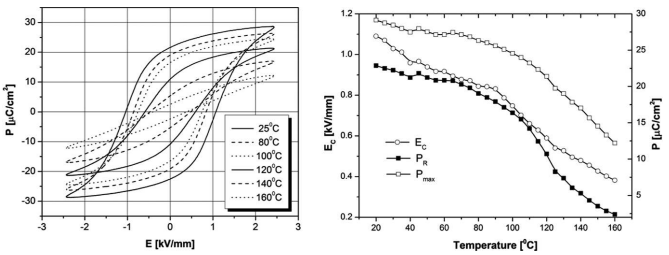


Fig. 4. Hysteresis loops of 0.690PMN-0.310PT sample of various temperatures and temperature dependence of the remanent polarization, maximum polarization and coercive field determined from loops

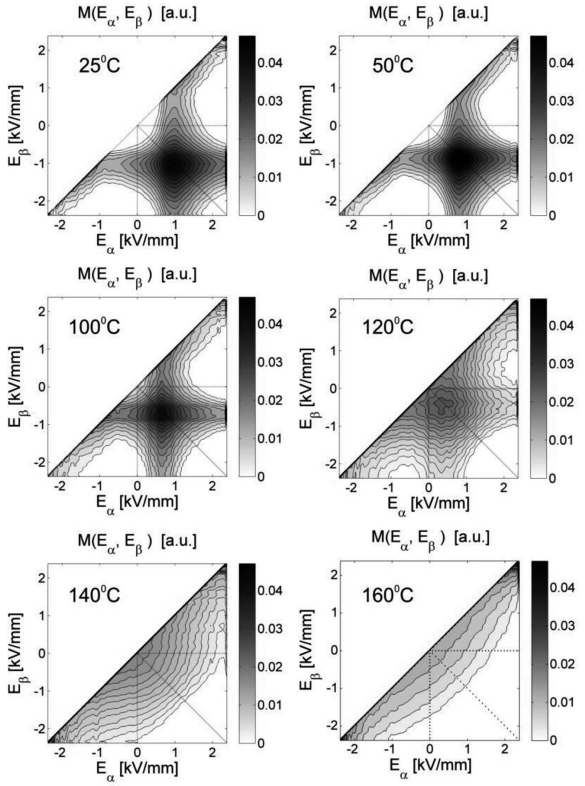


Fig. 5. Preisach distributions – temperature evolution for 0.690PMN-0.310PT sample

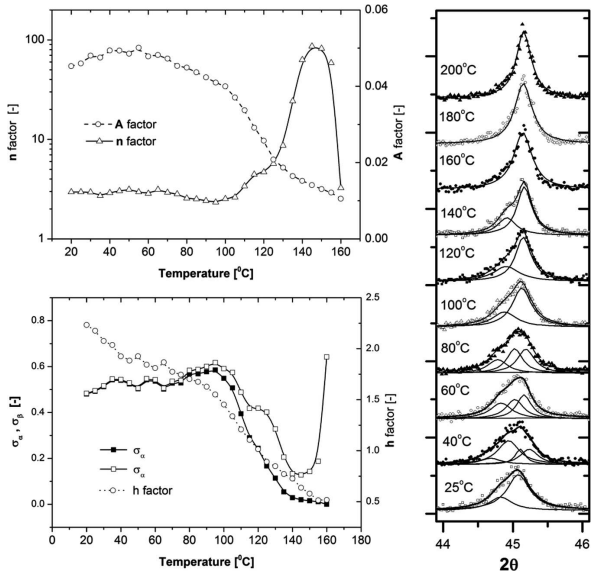


Fig. 6. Parameters obtained by fitting Preisach distributions using DAT function (left); XRD patterns of (200) reflection together with fitting results, circles – experimental data, lines – fitting results (right)

Comparing the parameters courses in Fig. 4 and 6, it can be seen that the coefficient $h$ (distribution maximum displacement) and coercive field $E_C$ are very similar. This property is repeated in all the comparative analysis.

Fig. 7 shows the summary results for the PMN-PT ceramic compositions obtained at room temperature. The power-law parameter $n$ reaching a maximum for the composition 0.075PT, points to a well-known fact that at room temperatures, compositions from range (0.07-0.1)PT lie on the boundary between rhombohedral and cubic phases [11], [12]. Parameters $E_C$, $P_R$ are not as sensitive to changes in sample structure. Adj $R^2$ coefficient, gives information about the quality of fit of the model to the experimental data, on the whole range studied compositions and temperatures remain within reasonable limits as shown in the Fig. 7.

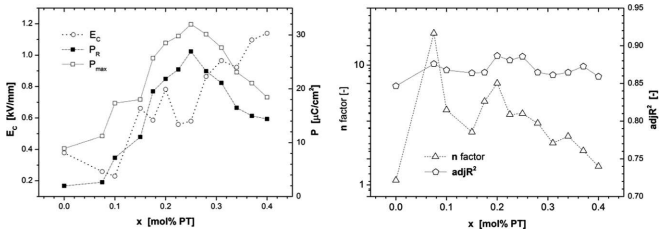


Fig. 7. Dependencies of parameters from hysteresis loops (left), and obtained by nonlinear fitting hysteresis loops using DAT function

## 6. Conclusion

This paper presents the identification of the Preisach distribution function using a relatively new iterative method based on single measurements of saturated ferroelectric hysteresis loops obtained from ceramic samples $(1\text{-}x)Pb(Mg_{1/3}Nb_{2/3})O_3\text{–}xPbTiO_3$ ($x$ = 0 to 0.40). The proposed enhanced, iterative method, allows to easily get the Preisach distributions with relatively simple measurements in the Sawyer-Tower testing system. Work also proposes to apply CPM to obtain additional information from the ferroelectric hysteresis loop, which cannot be seen by examining courses of classical parameters like $E_C$, $P_R$. For calculating these additional coefficients was proposed the use of DAT analytical model which can be used in a wide range of both temperature and chemical composition of ceramics.

REFERENCES

[1] F. Preisach, Z. Für, Phys. **94**, 277 (1935).
[2] I.D. Mayergoyz, Mathematical Models of Hysteresis and their Applications, 2nd ed., Academic Press, 32 (2003).
[3] D. Hughes, J.T. Wen, Smart Mater. Struct. **6**, 3, 287 (1997).
[4] P. Ge, M. Jouaneh, Precis. Eng. **20**, 2, 99 (1997).
[5] H. Ikeda, Y. Kadota, T. Morita, Jpn. J. Appl. Phys. **51**, 09MD01 (2012).
[6] R. Skulski, P. Wawrzała, K. Ćwikiel, D. Bochenek, J. Intell. Mater. Syst. Struct. **18**, 10, 1049 (2007).
[7] R. Skulski, P. Wawrzała, M. Szymonik, Arch. Met. Mater. **54**, 4, 935 (2009).
[8] W.S. Cleveland, J. Am. Stat. Assoc. **74**, 368, 829 (1979).
[9] A. Sutor, S.J. Rupitsch, R. Lerch, Appl. Phys. **100**, 2, 425 (2010).
[10] A.K. Singh, D. Pandey, Phys. Rev. B **67**, 6, 064102 (2003).
[11] T.R. Shrout, Z.P. Chang, N. Kim, S. Markgraf, Ferroelectr. Lett. Sect. **12**, 3, 63 (1990).
[12] B. Noheda, D.E. Cox, G. Shirane, J. Gao, Z.G. Ye, Phys. Rev. B **66**, 5, 054104 (2002).

*Received: 20 September 2013.*